

Moment Generating Function Based Performance Analysis of Maximal-Ratio Combining Diversity Receivers in the Generalized-K Fading Channels

Vivek K. Dwivedi · G. Singh

Published online: 4 February 2014
© Springer Science+Business Media New York 2014

Abstract In this paper, we have analyzed the performance of maximal ratio combining (MRC) diversity receiver of the wireless communication systems over the composite fading environment, which is modelled by using the generalized-K distribution. However, this distribution has been considered as a versatile distribution for the precise modelling of a great variety of the short-term fading in conjunction with the long-term fading (shadow fading) channel conditions. In this proposed analysis, we have derived the mathematical expression for the moment generating function (MGF) of the generalized-K fading channel model that is used to evaluate a novel closed-form expression of the average bit error rate for (BER) the binary phase-shift keying /binary frequency-shift keying and average symbol error rate (SER) for the rectangular quadrature amplitude modulation scheme. We have also derived the mathematical expressions for the outage probability as well as the channel capacity for the generalized-K fading channel model.

Keywords Generalized-K distribution · Multipath fading/shadow fading · Bit error rate · Maximal ratio combining diversity · Outage probability · Channel capacity · Symbol error rate

1 Introduction

The performance analysis of digital wireless communication systems usually deal with complicated and cumbersome statistical task. In general, the wireless communication channels are modelled as the mixture of path-loss variance with distance and multipath fading or shadow fading (long-term fading). The multipath fading is modelled by using the Rayleigh, Rician or

V. K. Dwivedi
Department of Electronics and Communication Engineering, Jaypee Institute of Information Technology,
Noida 201 307, India

G. Singh (✉)
Department of Electronics and Communication Engineering, Jaypee University of Information
Technology, Waknaghat, Solan 173 234, India
e-mail: drghanshyam.singh@yahoo.com

Nakagami distributions [1,2] and the shadow fading by using the lognormal distribution [1]. However, the multipath fading and shadow fading occur simultaneously in several cases and leads to the composite fading. Recent studies on the fading channels suggest that the composite multipath fading/shadow fading model is a better approximation in real-life scenarios of the wireless communication [3–11]. The composite Rayleigh-lognormal (R-L) distributions [3] is widely adopted to model the mixture of multipath fading and shadow fading [3–7]. It is well known fact that the Rayleigh-lognormal (Suzuki) distribution is a mixture of the Rayleigh and lognormal distribution, however it has a complicated integral form. However, the lack of general acceptance of this distribution may have been caused by its complicated integral form [6–8]. Therefore, an alternative approach which is mathematically more versatile to describe the mixture of multipath fading and shadow fading such as generalized-K distribution [5] or K-distribution [6,7] has been explored. In [6], it has been demonstrated that the Rayleigh-lognormal and K-distributions are similar, but the latter has a simpler form. Moreover, the existence of numerous analytic results regarding Bessel functions makes it possible to obtain closed-form solutions for the calculation of bit error rates, diversity effects etc. using the K-distribution, which is mixture of the Rayleigh and gamma distributions [7]. This distribution is simpler and thus more appropriate for the analysis and design of wireless communication systems.

Various mathematical expressions for the statistics of these diversity receivers, including the PDF (probability density function), MGF and the moments output signal-to-noise ratio (SNR) have been derived. Recently, few contributions dealing with the generalized-K and K-distribution with diversity combining have been reported in detail in [8,9]. In [8], the performance analysis of diversity combining techniques over the generalized-K fading channel has been explored, however the closed-form mathematical expression for the BER is not discussed. In [9], the performance of generalized selection combining (GSC) diversity receivers over K-fading channel is presented but the mathematic expression derived in [9] for the marginal moment generating function (MMGF) is not used to obtain the BER for M-array phase shift keying (MPSK). Bithas et al. [10] have presented the detail performance analysis for the important diversity receivers such as MRC, equal gain combining (EGC), selection combining (SC), and switch and stay combining (SSC) diversity operating over the composite fading channel modelled by using the generalized-K distribution. In [11], Bithas et al have also provided a novel closed-form mathematical expression for the Shannon's channel capacity and BER over several coherent and non-coherent digital modulation schemes. In [12,13], the authors have presented the channel capacity under different adaptive transmission policies, namely, optimal rate adaptation with constant transmitted power, optimal simulation power and rate adaptation, total channel inversion with fixed rate, and truncated channel inversion with fixed rate. For the results presented in [12], the authors consider an arbitrary chosen values of k (the Gamma distribution for the received average power due to the shadow fading) like the integer values of k or k equal to an integer plus one and half, however restricted over m (Nakagami fading parameters) only to the integer values. Efthymoglou et al. [13] have derived the closed-form analytical expressions operating over generalized-K fading channel for the outage probability, the average BER of several modulation schemes and the channel capacity under different transmission policies in terms of generalised hypergeometric functions that can be easily evaluated for wide range of fading values. However, for some special values of the fading parameters that is for the integer values of $(k - m)$, some of the functions in the formulae are not defined. In [14], the authors have developed a comprehensive framework for the analysis of channel capacity over generalized fading channels provided that the MGF of the received SNR is known in closed form and suggested that there are several cases of interest in which truly closed-form results may be obtained

by using this frameworks, for example, there are several scenarios in which the MGF of the received SNR can conveniently be expressed in terms of a Meijer-G function.

In this paper, we have exploited the MGF based performance analysis of the generalized-K fading channel with L —branch MRC diversity receiver over various modulation schemes. The main contribution of this paper consists of the evaluation of MGF function, which is used to obtain the closed-form mathematical expressions for average error rates, outage probability and channel capacity. However, the derived mathematical results are in terms of well known hypergeometric function and Meijer-G function, which can be implemented easily by using Maple or Mathematica simulation tool. However, the evaluation of average SER for rectangular M-QAM modulation scheme is solved uniquely. The remainder of the paper is organized as follows. Section 2 describes the proposed channel model of the wireless communication system. In Sect. 3, the mathematical expression for the MGF, average BER, average SER, outage probability and channel capacity have been derived for the proposed model. The numerical results are discussed in the Sect. 4. Finally, the Sect. 5 concludes the work.

2 Generalized-K Fading Channel Model

When the fading environment is such that the maximum delay spread of the channel is significantly large compared to the symbol time that is the frequency selective fading, then there exist multiple resolvable paths (the maximum number of which is determined by the ratio of the maximum delay spread to the symbol time) which result multiple channel reception. For the generic case of the multi-channel reception, the diversity combining schemes can be employed at the receiver to improve the SNR and thus the average BER performance. In general, the diversity combining schemes are rely on the characteristics of modulation and their associated detections. For coherent detection, the optimum form of diversity combining is the maximal ratio combining scheme. In the generalized-K fading environment, PDF of the output SNR is given by [11, 12]:

$$f_{\gamma}(\gamma) = \frac{2(\gamma)^{(\alpha'-1)/2}}{\Gamma(m)\Gamma(k)} (\Xi)^{(\alpha'+1)/2} K_{\beta'} \left[2\sqrt{\Xi\gamma} \right] \quad \gamma \geq 0 \quad (1)$$

where k and m are the distribution shaping parameters for the shadow fading and Nakagami parameter for the short-term fading associated with the channel, respectively. $\alpha' = m + k - 1$ and $\beta' = k - m$. $K_{\beta'}(\cdot)$ is the β' order modified Bessel function of the second kind [15, Equation (8.432.1)]. $\Gamma(\cdot)$ is the Gamma function [15, Equation (8.310.1)], $\Xi = (km)/\bar{\gamma}$ and $\bar{\gamma}$ is the corresponding average received SNR per bit. The PDF of instantaneous SNR at the output of a maximal ratio combiner with L -identical branches is obtained by substituting m with Lm and $\bar{\gamma}$ with $L\bar{\gamma}$ in Eq. (1) as given in [12]:

$$f_{\gamma}(\gamma) = \frac{2(\gamma)^{(\alpha-1)/2}}{\Gamma(mL)\Gamma(k)} (\Xi)^{(\alpha+1)/2} K_{\beta} \left[2\sqrt{\Xi\gamma} \right] \quad \gamma \geq 0 \quad (2)$$

where $\alpha = mL + k - 1$ and $\beta = k - mL$. For the diversity technique consideration, it is assumed that the distance among the diversity branches are significantly small. Furthermore, it is well known fact that the shadow fading occurs in the large geographical areas. Thus, it is reasonable to assume that the shadow fading effects are not de-correlated. Therefore, the shadow fading parameters k has been assumed equal for all the diversity branches.

3 Performance Analysis

The proposed model in this paper corresponds to the Nakagami-Gamma composite distribution which is controlled by two distribution shaping parameters m (Nakagami parameters for the short-term fading) and k (parameter of the Gamma distribution for the received average power due to the shadow fading). The parameter $m \geq 1/2$ inversely reflects the fading severity and the positive parameter k inversely reflects the shadow fading severity, which has been discussed in detail in [5]. The K-distribution is derived as a special case of the generalized-K distribution by considering $m = 1$.

3.1 Moment Generating Function

MGF is one of the most important characteristics of any distribution function because it is used for the average error rate performance evaluation of the wireless communication systems. However, it is clearly shown in [1] that MGF can be used to obtain the average BER of various modulations scheme (with and without diversity) either in the closed-form or in the form of a simple finite-range integral. Therefore, the MGF is a key tool that needs to be derived and is defined as [1]:

$$M_\gamma(s) = \int_0^\infty \exp(-s\gamma) f_\gamma(\gamma) d\gamma \tag{3}$$

By substituting the value of $f_\gamma(\gamma)$ from Eq. (2) into Eq. (3), the MGF of generalized-K fading channel can be written as:

$$M_\gamma(s) = \frac{(\Xi/s)^{\frac{\alpha+1}{2}}}{\Gamma(mM)\Gamma(k)} G_{2\ 1}^{2\ 1} \left[\frac{\Xi}{s} \middle| \begin{matrix} (1-\alpha)/2 \\ \beta/2 \end{matrix} \right] -\beta/2 \tag{4}$$

where $G(\cdot)$ is the Meijer-G function [15, Equation (9.301)], which is easy to evaluate by using the modern mathematical tools such as Mathematica and Maple. The detailed derivation of Eq. (4) is shown in ‘‘Appendix 6’’.

3.2 Computation of Error-Rates for Various Modulation Schemes

The average BER is an important property of the digital communication systems, which provides a base-line for the amount of information transferred and depends on the channel as well as modulation format. However, the average BER computation depends basically on the SNR at the receiver [17]. The average BER performance can be obtained by using MGF based approach. The mathematical expression for the average BER computation by using MGF based approach for BPSK/BFSK modulation format is [1,2]:

$$\bar{P}_b = \frac{1}{\pi} \int_0^{\pi/2} M_\gamma \left(\frac{g}{\sin^2 \theta} \right) d\theta \tag{5}$$

where g is the constant associated with modulation scheme. $g = 1$ for BPSK, $g = 1/2$ for coherent detection of BFSK and $g = 0.715$ for the coherent detection of minimum shift keying [2]. Therefore, the average BER for BPSK/ BFSK modulation scheme can be expressed as:

$$\bar{P}_b = \frac{(\Xi/g)^{\frac{\alpha+1}{2}}}{2\sqrt{\pi}\Gamma(mL)\Gamma(k)} G_{2,2}^{2,3} \left[\frac{\Xi}{g} \middle| \begin{matrix} -\alpha/2 & (1-\alpha)/2 \\ \beta/2 & -\beta/2 & -(1+\alpha)/2 \end{matrix} \right] \tag{6}$$

For $L = 1$ the Eq. (6) is similar with the [10, Equation (8)]. However, the detailed proof of Eq. (6) is given in ‘‘Appendix 7’’.

The average BER for differentially coherent detection of the phase-shift-keying (DPSK) or non-coherent detection of orthogonal frequency-shift-keying (NFSK) [1,2] is given as:

$$\bar{P}_{dpsk} = \frac{1}{2} M_\gamma(a) \tag{7}$$

where $a = 1$ for DPSK, $a = 1/2$ for NCFSK as given in [1,2] and $M_\gamma(\cdot)$ is the MGF. The average SER for rectangular M-QAM scheme by using the MGF based approach has been obtained as given in [18].

$$\bar{P}_{qam} = \frac{4}{\pi} \left(1 - \frac{1}{\sqrt{M}}\right) \int_0^{\frac{\pi}{2}} M_\gamma\left(\frac{g_{QAM}}{\sin^2 \theta}\right) d\theta - \frac{4}{\pi} \left(1 - \frac{1}{\sqrt{M}}\right)^2 \int_0^{\frac{\pi}{4}} M_\gamma\left(\frac{g_{QAM}}{\sin^2 \theta}\right) d\theta \tag{8}$$

where $g_{QAM} = 3/2(M - 1)$. However, the constellation size is given by $M = 2^\nu$ with ν is an even number. Equation (8) is consists of two integrals such as:

$$I_2 = \int_0^{\frac{\pi}{2}} M_\gamma\left(\frac{g_{QAM}}{\sin^2 \theta}\right) d\theta \tag{9}$$

and

$$I_3 = \int_0^{\frac{\pi}{4}} M_\gamma\left(\frac{g_{QAM}}{\sin^2 \theta}\right) d\theta \tag{10}$$

The integral I_2 as given in Eq. (9) can be solved as I_1 , which is given in ‘‘Appendix 7’’. Equation (10) can be further expressed as:

$$I_3 = \frac{1}{2\sqrt{2}} \left[\frac{\Gamma(-\beta)}{\Gamma(1/2 - \beta/2 + \alpha/2)} \left(\frac{\Xi}{2g_{QAM}}\right)^{(\alpha+\beta+1)/2} I_4 + \frac{\Gamma(\beta)}{\Gamma(1/2 + \beta/2 + \alpha/2)} \left(\frac{\Xi}{2g_{QAM}}\right)^{(\alpha-\beta+1)/2} I_5 \right] \tag{11}$$

where

$$I_4 = \sum_{n=0}^{\infty} \frac{1}{n!} \frac{\Gamma[(\alpha + \beta + 1)/2 + n]}{\Gamma[(\beta + \alpha + 1)/2]} \frac{\Gamma(\beta + 1)}{\Gamma(\beta + 1 + n)} \left(\frac{\Xi}{2g_{QAM}}\right)^n \times B\left(n + \frac{\alpha + \beta + 2}{2}, 1\right) \times F\left(1/2, n + (\alpha + \beta + 2)/2, n + (\alpha + \beta + 4)/2, 1/2\right) \tag{12}$$

$$I_5 = \sum_{n=0}^{\infty} \frac{1}{n!} \frac{\Gamma[(\alpha - \beta + 1)/2 + n]}{\Gamma[(\alpha - \beta + 1)/2]} \frac{\Gamma(\beta + 1)}{\Gamma(\beta + 1 + n)} \left(\frac{\Xi}{2g_{QAM}}\right)^n \times B\left(n + \frac{\alpha - \beta + 2}{2}, 1\right) \times F\left(1/2, n + (\alpha - \beta + 2)/2, n + (\alpha - \beta + 4)/2, 1/2\right) \tag{13}$$

The detailed proof of Eq. (11) is shown in ‘‘Appendix 8’’. By substituting the value of I_3 from the Eq. (11) and the value of I_2 from Eq. (9) in Eq. (8), then the average SER of the rectangular M-QAM can be expressed as:

$$\begin{aligned} \bar{P}_{qam} = & \frac{2}{(\pi)^{3/2}} \left(1 - \frac{1}{\sqrt{M}}\right) \frac{(\Xi/g_{QAM})^{(1+\alpha)}}{\Gamma(mL)\Gamma(k)} G_{2\ 2}^{2\ 3} \left[\frac{\Xi}{g_{QAM}} \middle| \begin{matrix} -\alpha/2 & (1-\alpha)/2 \\ \beta/2 & -\beta/2 - (\alpha+1)/2 \end{matrix} \right] \\ & - \frac{\sqrt{2}}{\pi} \left(1 - \frac{1}{\sqrt{M}}\right)^2 \times \left[\frac{\Gamma(-\beta)}{\Gamma(1/2 - \beta/2 + \alpha/2)} \left(\frac{\Xi}{2g_{QAM}}\right)^{(\alpha+\beta+1)/2} I_4 \right. \\ & \left. + \frac{\Gamma(\beta)}{\Gamma(1/2 + \beta/2 + \alpha/2)} \left(\frac{\Xi}{2g_{QAM}}\right)^{(\alpha-\beta+1)/2} I_5 \right] \end{aligned} \tag{14}$$

Equation (14) is a novel mathematical expression for the average SER over the generalized-K fading channel with L —branch MRC diversity receiver, which is simply evaluate by using Mathematica and Maple.

3.3 Outage Probability

The outage probability (P_{out}) is defined as the probability that the instantaneous error rate exceeds a specified value or equivalently that combined the SNR falls below a certain threshold, γ_{th} , [1, 2, 19]. In other words, P_{out} is the cumulative distribution function (CDF) of γ which is evaluated at certain threshold value. However, an approach to obtain the outage probability is: 1) find the PDF of γ and 2) integrate it over that PDF as given in:

$$P_{out} = \int_0^{\gamma_{th}} f(\gamma) d\gamma, \tag{15}$$

By using Eq. (2) and after some mathematical manipulation, the outage probability, P_{out} can be expressed as:

$$P_{out} = 1 - \int_{\gamma_{th}}^{\infty} \frac{2(\gamma)^{(\alpha-1)/2}}{\Gamma(mL)\Gamma(k)} (\Xi)^{(\alpha+1)/2} K_{\beta} \left[2\sqrt{\Xi\gamma} \right] d\gamma \tag{16}$$

Now, the Eq. (16) can be expressed as:

$$P_{out} = 1 - \frac{(\Xi\gamma_{th})^{(\alpha+1)/2}}{\Gamma(mL)\Gamma(k)} G_{1\ 3}^{3\ 0} \left[\Xi\gamma_{th} \middle| \begin{matrix} 1 - (\alpha + 1)/2 \\ -(\alpha + 1)/2 & \beta/2 & -\beta/2 \end{matrix} \right] \tag{17}$$

This is the closed-form mathematical expression for the outage probability involving Meijer-G function, which is simply evaluated by using Mathematica and Maple. The detailed proof of Eq. (17) is presented in ‘‘Appendix 9’’.

3.4 Channel Capacity By Channel Inversion with Fixed Rate

The interest stems for the fact that Shannon’s channel capacity represents the upper bound for the data rate achievable in a transmission with an arbitrary small error probability, which serves as an ultimate performance measure of the communication system. In this section, a closed-form mathematical expression for the channel capacity with power adaptive transmission technique for the generalized-K fading channel model by using MGF is presented.

The channel capacity by channel inversion with fixed rate (C_{CIFR}) requires that the transmitter exploits the channel state information such that the constant SNR is maintained at receiver. This technique uses fixed-rate modulation and fixed code design, since the channel after channel inversion appears as a time-invariant additive white Gaussian noise (AWGN) channel. As a result, the channel inversion with fixed rate is the least complex technique to implement, however better channel informations are available at the transmitter and receiver. The channel capacity per unit bandwidth of the fixed channel inversion with fixed rate in terms of MGF can be expressed as [14, 19]:

$$C_{CIFR} = \log_2 \left(1 + \frac{1}{\int_0^\infty M_\gamma(s) ds} \right) \tag{18}$$

By using Eq. (18), the channel capacity can be expressed as:

$$C_{CIFR} = \log_2 \left(1 + \frac{\Gamma(mL)\Gamma(k)}{\Xi\Gamma((\alpha + \beta - 1)/2)\Gamma((\alpha - \beta - 1)/2)} \right) \tag{19}$$

However, the detailed derivation of Eq. (19) is shown in ‘‘Appendix 10’’. Equation (19) is similar as [12, Equation (29)]. Therefore, the Eq. (19) is a general expression for the channel capacity per unit bandwidth for total channel inversion with MRC diversity receiver.

4 Results and Discussion

In this section, we have presented the results for performance evaluation of the proposed communication system by using the MGF based analysis as discussed in the preceding sec-

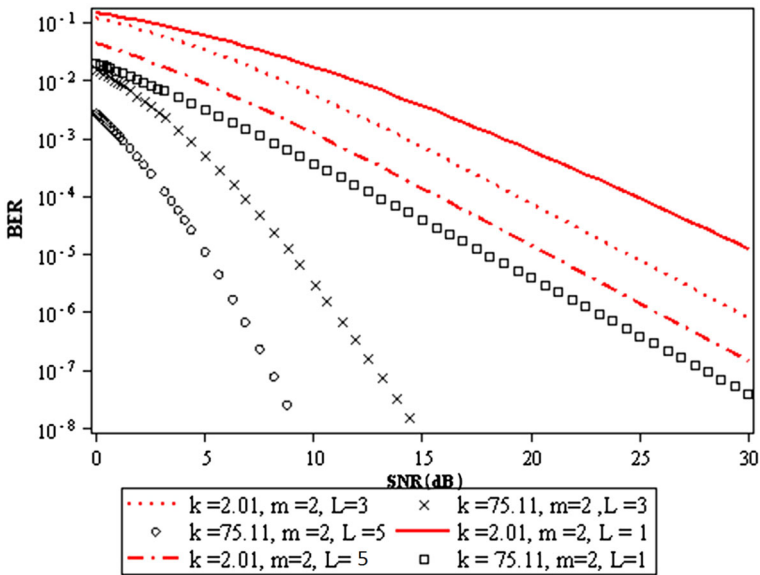


Fig. 1 The average BER versus SNR characteristics of BPSK modulation scheme over the generalized-K fading channel with L —branch MRC diversity receiver

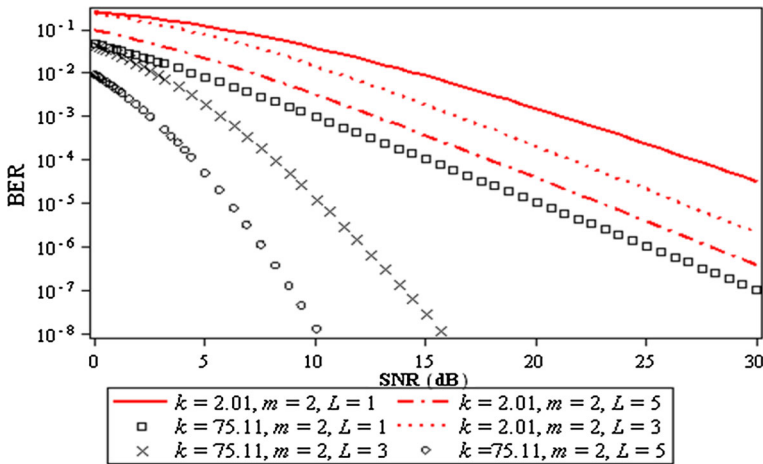


Fig. 2 The average BER versus SNR characteristics of DPSK modulation scheme over the generalized-K fading channel with L —branch MRC diversity receiver

tions for error rates, outage probability and channel capacity for various digital modulation formats. We have used the Eq. (6), (7) and (14) to obtain the average BER and average SER response, respectively. Equations (17) and (19) are used to obtain the outage probability and channel capacity, respectively. Figure 1 depicts the average BER versus the average SNR characteristics for the generalized-K fading channel with MRC diversity receiver. However, the MRC diversity receiver requires the individual signals from each branch which are weighted by their signal voltage to the noise power ratios and then summed coherently [1].

In this proposed analysis, we have assumed the perfect knowledge of branch amplitudes and phases that is the MRC diversity with perfect combining which is the optimal diversity scheme. Therefore it provides the maximum channel capacity improvement relative to all the diversity combining techniques. The average BER against the average received SNR per bit for BPSK modulation format in the fading channel conditions has been obtained by an appropriate choice of the shaping parameters k and m . For $k = 2.01$ as the diversity branches increases the average BER performance improves for the same values of SNR, however for $k = 75.11$ as the diversity branches increases the average BER performance improves more significantly than that at $k = 2.01$ as shown in Fig. 1. The Fig. 2 demonstrated that the average BER versus average SNR characteristics for DPSK modulation scheme over the generalized-K fading channel with L —branch MRC diversity receiver. However, with the increase of diversity branches, the error rate performance improves significantly but this improvement is slightly less than that of BPSK modulation scheme. Figure 3a, b show the comparison of average BER versus SNR characteristics between the proposed method with that reported in [8] for BPSK and DPSK modulation schemes over the generalized-K fading channel with L —branch MRC diversity receiver for $k = 2.2$ and $m = 1.5$, respectively. In Fig. 3a, we have compared equation (6) of the proposed method with [8, Equation (22)] for BPSK modulation scheme, and in Fig. 3b, we have compared equation (7) of the proposed method with [8, Equation (20)] for DPSK modulation scheme. It is clearly seen from Fig. 3a, b that the average BER versus SNR characteristics of the proposed method is almost similar to that reported in [8]. Figure 4 demonstrates the average SER versus SNR characteristics of 4-QAM modulation scheme. As the number of diversity branches increases for the chosen values of the distribution shaping parameters for the shadow fading and Nakagami parameter

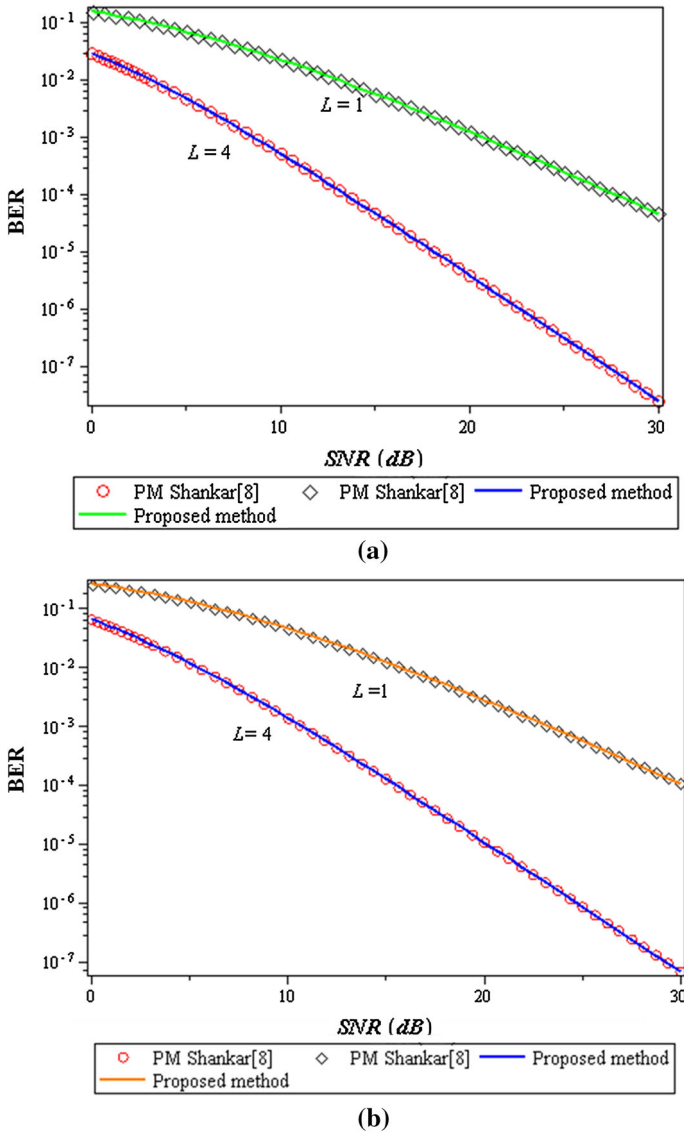


Fig. 3 Comparison of average BER versus SNR characteristics over generalized-K fading channel with L -branch MRC diversity receiver between the proposed method and that reported by Shanker [8] for **a** BPSK and **b** DPSK

for the short-term fading associated with the channel, the performance of the communication system improve. However, this improvement is more significant at $k = 7/2$ as compared to $k = 1/2$. However, the Eq. (14) is given in an infinite series form, which converges rapidly and steadily requiring very few terms for the desired accuracy. In analyzing the accuracy of the numerical results of Eq. (14), we are aware for the possible source of errors in each stage of the computational process and with the extent to which these errors can affect the device performance. The truncation error is caused when we are forced to use mathematical techniques that provide approximate results rather than exact. However, for the SNR greater

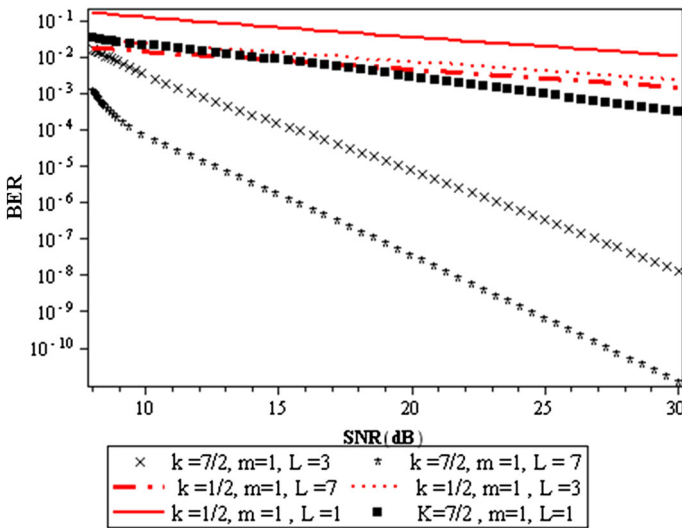


Fig. 4 The average SER versus SNR response for M-QAM modulation scheme over the generalized-K fading channel with L —branch MRC diversity receiver

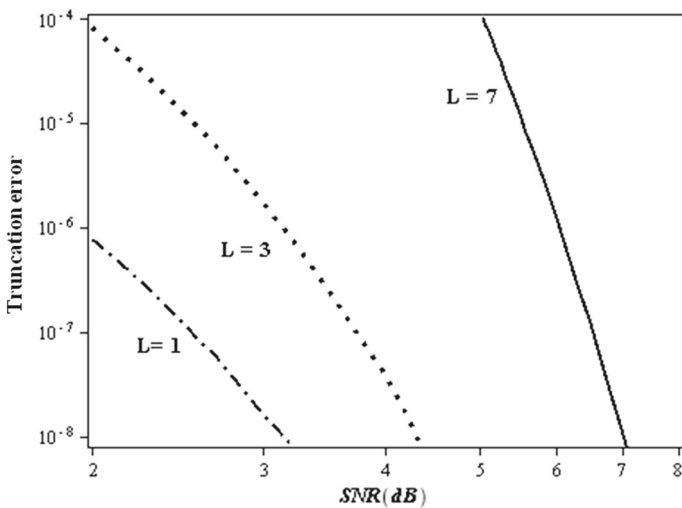


Fig. 5 The truncation error versus SNR ($k = 7/2, m = 1$) for various diversity branches

than 8 dB only two terms are required for the sufficient accuracy and when it is less than 8 dB. The Fig. 5 demonstrates the truncation error versus SNR response for the total number of terms in the series that is equal to 12. Form Fig. 5, it is illustrated that as the SNR increases, the truncation error decrease, however the truncation error increases with increase of the diversity branch at the receiver.

Figure 6 depicts the outage probabilities versus SNR characteristics for the generalized-K fading channel with L —branch MRC diversity receiver ($m = 2, L = 2$, threshold SNR (γ_{th}) = 15 and 10 dB) for the light shadow fading ($k = 75.11$) and heavy shadow fading ($k = 2.01$). However, for a given value of the threshold SNR, the outage probability decreases

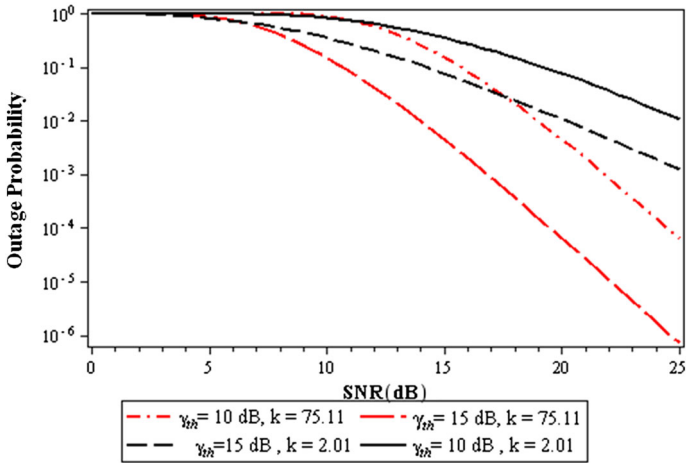


Fig. 6 The outage probability versus SNR characteristics for the generalized-K fading channel with L —branch MRC diversity receiver ($m = 2, L = 2$) for the light shadow fading ($k = 75.11$) and heavy shadow fading ($k = 2.01$)

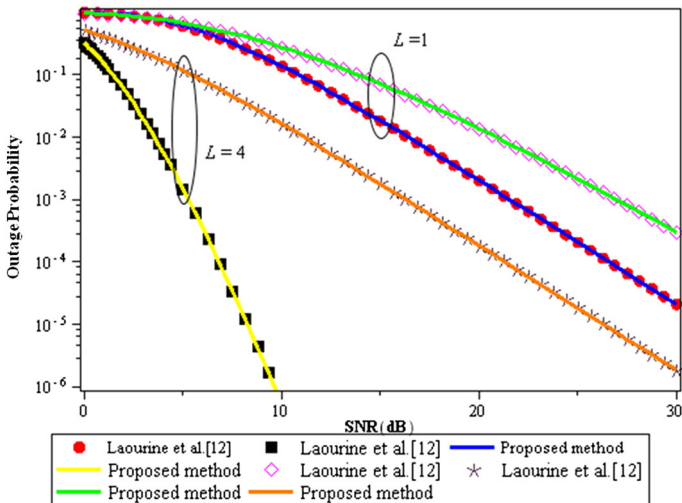


Fig. 7 Comparison of the outage probabilities versus SNR characteristics between the proposed method and Laourine et al. [12] for the generalized-K fading channel with L —branch MRC diversity receiver ($m = 2, L = 1$ and 4) for the light shadow fading ($k = 75.11$) and heavy shadow fading ($k = 2.01$)

with increase of the SNR for both light shadow fading as well as heavy shadow fading. However, this decrement is more significant in the light shadow fading as compared to that of the heavy shadow fading. As the values of the threshold SNR increases for the heavy shadow fading and light shadow fading, the outage probability decreases at chosen SNR. In Fig. 7, the comparison of outage probability versus SNR characteristics between the proposed method and other reported by Laourine et al. [12] for shaping parameter ($m = 2$), number of diversity receiver ($L = 1, 4$) and light as well as heavy shadow fading ($k = 75.11, 2.01$) has been discussed. We have compared the outage probability versus SNR characteristics between the proposed method of as in Eq. (17) and Laourine et al. [12, Equation (24)]. However,

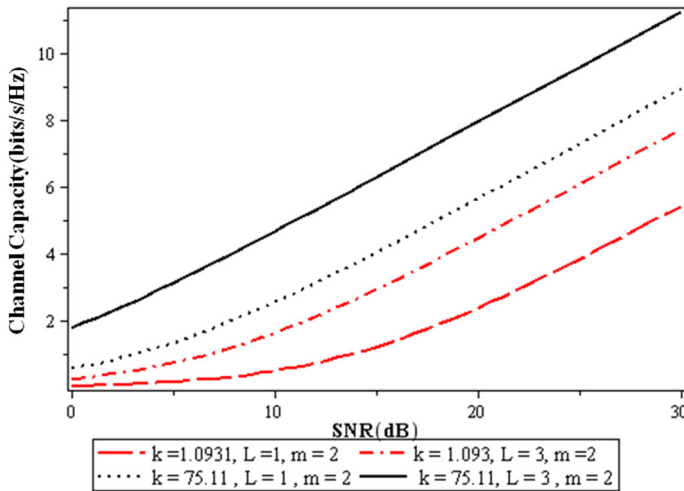


Fig. 8 The channel capacity per unit bandwidth for generalized-K fading channel for channel inversion with fixed rate versus SNR for the light shadow fading ($k = 75.11$) and heavy shadow fading ($k = 1.0931$)

the results of proposed method are closely matched with that of Laourine et al. [12]. The Fig. 8 demonstrate the channel capacity per unit bandwidth for the generalized-K fading channel for channel inversion with fixed rate (C_{CIFR}) versus SNR characteristics for the light shadow fading ($k = 75.11, m = 2$) and heavy shadow fading ($k = 1.0931, m = 2$) for several diversity branches ($L = 1, 3$). With emphasizing on the effect of shadow fading, particularly in case of the heavy shadow fading ($k = 1.0931$) the channel capacity degrades significantly as shown in Fig. 8 and it improves with the increase of the diversity branches because the channel inversion suffers relatively the largest capacity penalty, however the penalty diminishes with increase of the diversity. Although the diversity yields large capacity gain for all the techniques as d, however the gain is more pronounced with channel inversion since it is the least complex scheme to implement. However, there is a trade-off between the complexity and capacity for various adaptation methods and diversity combining techniques as discussed in [12, 13].

5 Conclusion

In this paper, we have presented a simple mathematical approach to yield a closed-form expression for the performance measurement of a generalized-K distribution fading channel by using simple MGF based approach. For this purpose, first we have obtained a MGF for the generalized-K fading channel with L —branch MRC diversity receiver. This mathematical expression of MGF is presented in terms of the Meijer- G function, which is used to evaluate BER of BPSK/BFSK modulation and SER of M-QAM schemes. However, the expression for average BER of BPSK/BFSK is given by Eq. (6), and for $L = 1$ the Eq. (6) is similar with that reported in [11, Equation (8)]. We have derived a novel mathematical equation (14) for the average SER over the generalized-K fading channel with L —branch MRC diversity receiver. Moreover, we have also derived the mathematical expressions for the outage probability and channel capacity for the channel inversion with fixed rate (C_{CIFR}). However, the C_{CIFR} is very easily computed by using MGF based approach, and for $L = 1$, C_{CIFR} is computed by

using Eq. (19) which is similar to that reported in [12, Equation (29)] and [13, Equation (27)]. The mathematical expressions provided in this paper are very useful for the assessment of the performance of the wireless digital communication system over the generalized-K fading environment. The proposed mathematical analysis is complemented by various performance evaluation results, which demonstrate the accuracy of the theoretical approach.

Acknowledgments The authors are sincerely thankful to the anonymous reviewers for their critical comments and suggestions to improve the quality of the manuscript.

6 Appendix: MGF of Generalized-K Fading Channel

Equation (4) can be obtained by substituting the value of $f_\gamma(\gamma)$ from Eq. (2) into Eq. (3) and the MGF of generalized K-fading channel can be written as:

$$M_\gamma(s) = \frac{2 (\Xi)^{(\alpha+1)/2}}{\Gamma(mL)\Gamma(k)} \int_0^\infty \exp(-s\gamma) (\gamma)^{(\alpha-1)/2} K_\beta \left[2\sqrt{\Xi\gamma} \right] d\gamma \tag{20}$$

By putting $K_\beta (2\sqrt{\Xi\gamma})$ as $\frac{1}{2} G_{0\ 2}^{2\ 0} \left[\Xi\gamma \mid \beta/2 \ -\beta/2 \right]$ [16, Equation (8.4.23.1)] in Eq. (20), we get:

$$M_\gamma(s) = \frac{(\Xi)^{(\alpha+1)/2}}{\Gamma(mL)\Gamma(k)} \int_0^\infty \gamma^{(\alpha-1)/2} e^{-s\gamma} G_{0\ 2}^{2\ 0} \left[\Xi\gamma \mid \beta/2 \ -\beta/2 \right] d\gamma \tag{21}$$

By putting $\int_0^\infty x^{s-1} e^{-\sigma x} G_{p\ q}^{m\ n} \left[\omega x \mid \begin{matrix} (a_p) \\ (b_q) \end{matrix} \right] dx = \sigma^{-s} G_{p+1\ q}^{m\ n+1} \left[\frac{\omega}{\sigma} \mid \begin{matrix} 1-s\ (a_p) \\ (b_q) \end{matrix} \right]$ form [16, Equation (2.24.3.1)] into Eq. (21) provides equation (4).

7 Appendix: Average BER for BPSK/BFSK Modulation Scheme

For the proof of Eq. (6), we assume, $I_1 = \int_0^{\pi/2} M_\gamma \left(\frac{g}{\sin^2\theta} \right) d\theta$ in Eq. (5). By using Eq. (4), I_1 can be expressed as:

$$I_1 = \frac{(\Xi)^{\frac{\alpha+1}{2}}}{\pi\Gamma(mL)\Gamma(k)} \int_0^{\frac{\pi}{2}} \left(\frac{g}{\sin^2\theta} \right)^{-\frac{(\alpha+1)}{2}} G_{1\ 2}^{2\ 1} \left[\frac{\Xi \sin^2\theta}{g} \mid \begin{matrix} (1-\alpha)/2 \\ \beta/2 \ -\beta/2 \end{matrix} \right] d\theta \tag{22}$$

By changing the variable $t = \sin^2\theta$ and after some mathematical manipulation, Eq. (22) can be expressed as:

$$I_1 = \frac{(\Xi/g)^{\frac{\alpha+1}{2}}}{2\pi\Gamma(mL)\Gamma(k)} \int_0^1 (t)^{\frac{\alpha}{2}} (1-t)^{-1/2} G_{1\ 2}^{2\ 1} \left[\frac{\Xi t}{g} \mid \begin{matrix} (1-\alpha)/2 \\ \beta/2 \ -\beta/2 \end{matrix} \right] dt \tag{23}$$

By using $\int_0^1 x^{s-1} (1-x)^{t-1} G_{p\ q}^m\ n \left[\omega x \left| \begin{matrix} (a_p) \\ (b_q) \end{matrix} \right. \right] dx = \Gamma(t) G_{p+1\ q+1}^m\ n+1 \left[\omega \left| \begin{matrix} 1-s\ (a_p) \\ (b_q)\ 1-s-t \end{matrix} \right. \right]$ from [16, Equation (2.24.2)], the Eq. (23) can be expressed as:

$$I_1 = \frac{(\Xi/g)^{\frac{(1+\alpha)}{2}} \sqrt{\pi}}{2\Gamma(mL)\Gamma(k)} G_{2\ 3}^2\ 2 \left[\frac{\Xi}{g} \left| \begin{matrix} -\alpha/2 & (1-\alpha)/2 \\ \beta/2 & -\beta/2 & -(\alpha+1)/2 \end{matrix} \right. \right] \tag{24}$$

By using Eqs. (5) and (24), we can obtain Eq. (6).

8 Appendix: Integration I3

To derive Eq. (11), we proceed by using [15, Equation (6.643.3)] and Eq. (2), the MGF of the generalized K-fading distribution can be expressed as:

$$M_Y(s) = \left(\frac{\Xi}{s}\right)^{\alpha/2} \exp\left(\frac{\Xi}{2s}\right) W_{-\alpha/2, \beta/2} \left(\frac{\Xi}{s}\right) \tag{25}$$

where $W_{-\mu, \nu}(\cdot)$ is the Whittaker function as discussed in [15, Equation (9.220.4)]. From Eq. (10) and (25), the integral I_3 can be expressed as:

$$I_3 = \int_0^{\frac{\pi}{4}} \left(\frac{\Xi \sin^2 \theta}{g_{QAM}}\right)^{\alpha/2} \exp\left(\frac{\Xi \sin^2 \theta}{2g_{QAM}}\right) W_{-\alpha/2, \beta/2} \left(\frac{\Xi \sin^2 \theta}{g_{QAM}}\right) d\theta \tag{26}$$

By using the transformation $t = 2 \sin^2 \theta$ and after some mathematical manipulation, the Eq. (26) can be written as:

$$I_3 = \frac{1}{2\sqrt{2}} \left(\frac{\Xi}{2g_{QAM}}\right)^{\alpha/2} \int_0^1 t^{(\alpha-1)/2} (1-t/2)^{-1/2} \exp\left(\frac{\Xi t}{4g_{QAM}}\right) W_{-\alpha/2, \beta/2} \left(\frac{\Xi t}{2g_{QAM}}\right) dt \tag{27}$$

With the help of [15, Equation (9.220.4)], [15, Equation (9.220.3)] and [15, Equation (9.220.2)] Eq. (27) can be expressed as:

$$\begin{aligned} I_3 = & \frac{1}{2\sqrt{2}} \left(\frac{\Xi}{2g_{QAM}}\right)^{\alpha/2} \int_0^1 t^{(\alpha-1)/2} (1-t/2)^{-1/2} \left[\frac{\Gamma(-\beta)}{\Gamma(1/2 - \beta/2 + \alpha/2)} \left(\frac{\Xi t}{2g_{QAM}}\right)^{(\beta+1)/2} \right. \\ & \times {}_1F_1\left(\frac{\alpha + \beta + 1}{2}, \beta + 1, \frac{\Xi t}{2g_{QAM}}\right) + \frac{\Gamma(\beta)}{\Gamma(1/2 + \beta/2 + \alpha/2)} \left(\frac{\Xi t}{2g_{QAM}}\right)^{(-\beta+1)/2} \\ & \left. \times {}_1F_1\left(\frac{\alpha - \beta + 1}{2}, \beta + 1, \frac{\Xi t}{2g_{QAM}}\right) \right] dt \end{aligned} \tag{28}$$

where, ${}_1F_1$ is the confluent hypergeometric function as discussed in [15, Equation (9.210.1)]. By using [15, Equation (9.210.1)] and [15, Equation (9.111)], Eq. (28) can be written as Eq. (11).

9 Appendix: Outage Probability

To derive Eq. (16), we proceed by substituting the value of $f_\gamma(\gamma)$ from Eq. (2) into Eq. (15), P_{out} can be expressed as:

$$P_{out} = 1 - \int_{\gamma_{th}}^{\infty} \frac{2(\gamma)^{(\alpha-1)/2}}{\Gamma(mL)\Gamma(k)} (\Xi)^{(\alpha+1)/2} K_\beta \left[2\sqrt{\Xi\gamma} \right] d\gamma \tag{29}$$

By replacing $K_\beta(\cdot)$ as ${}_{\frac{1}{2}}G_{0\ 2}^{2\ 0} \left[\Xi\gamma \mid \beta/2 \ -\beta/2 \right]$ from [16, Equation (8.4.23.1)] in Eq. (29), we get:

$$P_{out} = 1 - \frac{(\Xi)^{(\alpha+1)/2}}{\Gamma(mL)\Gamma(k)} \int_{\gamma_{th}}^{\infty} (\gamma)^{(\alpha-1)/2} G_{0\ 2}^{2\ 0} \left[\Xi\gamma \mid \beta/2 \ -\beta/2 \right] d\gamma \tag{30}$$

Now, with the help of $\int_u^\infty x^{s-1}(x-u)^{t-1} G_{p\ q}^{m\ n} \left[\omega x \mid \begin{matrix} (a_p) \\ (b_q) \end{matrix} \right] dx = \Gamma(t) G_{p+1\ q+1}^{m+1\ n}$ $\left[\omega \mid \begin{matrix} (a_p) \ 1-s \\ 1-s-t \ (b_q) \end{matrix} \right]$ from [16, Equation (2.24.2.3)], the Eq. (30) can be expressed as Eq. (16).

10 Appendix: Channel Capacity by Channel Inversion with Fixed Rate

To derive Eq. (19), we proceed by assuming, $I_6 = \int_0^\infty M_\gamma(s) ds$ in Eq. (18). Using Eq. (4) I_6 can be expressed as:

$$I_6 = \int_0^\infty \frac{(\Xi/s)^{\frac{\alpha+1}{2}}}{\Gamma(mL)\Gamma(k)} G_{1\ 2}^{2\ 1} \left[\frac{\Xi}{s} \mid \begin{matrix} (1-\alpha)/2 \\ \beta/2 \ -\beta/2 \end{matrix} \right] ds \tag{31}$$

By putting $1/s = t$ in Eq. (31) and using [15, Equation (7.811.4)], Eq. (31) can be written as:

$$I_6 = \frac{\Xi \Gamma((\alpha + \beta - 1)/2) \Gamma((\alpha - \beta - 1)/2)}{\Gamma(mL) \Gamma(k)} \tag{32}$$

If we substitute value of I_6 from Eq. (32) to Eq. (18) it results Eq. (19).

References

1. Simon, M. K., & Alouini, M.-S. (2005). *Digital communication over fading channels* (2nd ed.). New York: Wiley.
2. Dwivedi, V. K., & Singh, G. (2011). A novel moment generating function based performance analysis over correlated Nakagami-m fading. *Journal of Computational Electronics*, 10(4), 373–381.
3. Suzuki, H. (1977). A statistical model for urban radio propagation. *IEEE Transactions on Communication*, 25(7), 673–680.
4. Hansen, F., & Meno, F. I. (1977). Mobile fading-Rayleigh and Lognormal superimposed. *IEEE Transactions on Vehicular Technology*, 26(4), 332–335.
5. Shankar, P. M. (2004). Error rates in generalized shadowed fading channels. *Wireless Personal Communications*, 28(4), 233–238.
6. Abdi, A., & Kaveh, M. (1998). K distribution: An appropriate substitute for Rayleigh-Lognormal distribution in fading-shadow fading wireless channels. *Electronics Letters*, 34(9), 851–852.

7. Abdi, A., & Kaveh, M. (2000). Comparison of DPSK and MSK bit error rates for K and Rayleigh-Lognormal fading distributions. *IEEE Communications Letters*, 4(4), 122–124.
8. Shankar, P. M. (2006). Performance analysis of diversity combining algorithms in shadowed fading channels. *Wireless Personal Communications*, 37(1–2), 61–72.
9. Theofilakos, P., Kanatas, A. G., & Efthymoglou, G. P. (2008). Performance of generalized selection combining receivers in K fading channels. *IEEE Communications Letters*, 12, 816–818.
10. Bithas, P. S., Mathiopoulos, P. T., & Kotsopoulos, S. A. (2007). Diversity reception over generalized- K (K_G) fading channels. *IEEE Transactions on Wireless Communication*, 6(12), 4238–4243.
11. Bithas, P. S., Sagias, N. C., Mathiopoulos, P. T., Karagiannidis, G. K., & Rontogiannis, A. A. (2006). On the performance analysis of digital communications over generalized- K fading channels. *IEEE Communications Letters*, 5(10), 353–355.
12. Laourine, A., Alouini, M.-S., Affes, S., & Stephenne, A. (2008). On the capacity of generalized- K fading channels. *IEEE Transactions on Wireless Communications*, 7(7), 2441–2445.
13. Efthymoglou, G. P., Ermolova, N. Y., & Aalo, V. A. (2010). Channel capacity and average error rates in generalized- K fading channels. *IET Communications*, 4(11), 1364–1372.
14. DiRenzo, M., Graziosi, F., & Santucci, F. (2010). Channel capacity over generalized fading channels: A novel MGF-based approach for performance analysis and design of wireless communication systems. *IEEE Transactions on Vehicular Technology*, 59, 127–149.
15. Gradshteyn, I. S., & Ryzhik, I. M. (2007). *Table of integrals, series, and products* (7th ed.). New York: Academic.
16. Prudnikov, A. P., Brychkov, Y. A., & Marichev, O. I. (1990). *Integrals and series: More special functions*. Gordon and Breach Science, vol. 3, translated from the Russian by G. G. Gould.
17. Dwivedi, V. K., & Singh, G. (2011). Error-rate analysis of the OFDM for correlated Nakagami- m fading channel by using maximal-ratio combining diversity. *International Journal of Microwave and Wireless Technology*, 3(6), 717–7263.
18. Simon, M. K., & Alouini, M.-S. (1999). A unified approach for calculating error rates of linearly modulated signals over generalized fading channels. *IEEE Transactions on Communications*, 47, 1324–1333.
19. Dwivedi, V. K., & Singh, G. (2012). Marginal moment generating function based analysis of channel capacity over correlated Nakagami- m fading with maximal-ratio combining diversity. *Progress in Electromagnetic Research B*, 41, 333–356.



Vivek K. Dwivedi received B.E. from the RGPV, Bhopal, India in 2003 and Master of Engineering from Birla Institute of Technology, Mesra, Ranchi, India in 2006 and completed his Ph.D. in Electronics and Communication Engineering from Jaypee University of Information Technology, Waknaghat, Solan, India in 2012. Currently, he is working Assistant Professor, in the Department of Electronics and Communication Engineering in Jaypee Institute of Information Technology, Noida, India. He has authored more than 22 research papers of referred Journals and International conferences. His area of research is OFDM systems, fading in wireless channel and cognitive radio.



G. Singh received Ph.D. degree in electronics engineering from the Indian Institute of Technology, Banaras Hindu University (IIT-BHU), Varanasi, India, in 2000. He was associated with Central Electronics Engineering Research Institute, Pilani, and Institute for Plasma Research, Gandhinagar, India, respectively, where he was Research Scientist. He has also worked as an Assistant Professor at Electronics and Communication Engineering Department, Nirma University of Science and Technology, Ahmedabad, India. He was a Visiting Researcher at the Seoul National University, Seoul, S. Korea. At present, he is working as Professor with the Department of Electronics and Communication Engineering, Jaypee University of Information Technology, Wakanaghat, Solan, India. He is the author/co-author of more than 170 scientific papers of the refereed Journal and International/National Conferences. His research interests include microwave/THz antennas and its potential applications, surface-plasmons, Electromagnetics and its applications, nanophotonics, and next generation communication systems. He is author/co-

author of two books, “Terahertz Planar Antennas for Next Generation Communication” and “MOSFET Technologies for Double-Pole Four-Through Radio-Frequency Switch” which is published by Springer International Publishing.